

ROYAL AIR FORCE ESTABLISHMENT C.P. No. 1175
BEDFORD.



MINISTRY OF DEFENCE
AERONAUTICAL RESEARCH COUNCIL
CURRENT PAPERS

Pitot-Stem Blockage Corrections in Uniform and Non-Uniform Flow

by

R. W. F. Gould
Aerodynamics Division NPL

LONDON · HER MAJESTY'S STATIONERY OFFICE

1971

Price 42½p net

August-1970

Pitot-stem Blockage Corrections in Uniform
and Non-uniform Flow

- By -

R. W. F. Gould,
Aerodynamics Division, NPL

SUMMARY

Wind tunnel measurements are described which determine the error introduced into static pressure measurements in a pipe or duct by the presence of a pitot (or other) stem downstream of the plane of measurement. The effects measured in a uniform stream are used to calculate corresponding stem-blockage corrections in non-uniform flow.

The method is applied to fully developed pipe flow measurements in circular and rectangular ducts.

List of Contents

	<u>Page</u>
1. List of Symbols	2
2. Introduction	3
3. Measurement of the Blockage Effect due to a Stem of Circular Section	4
3.1 Experimental method	4
3.1(a) Basis of method	4
3.1(b) Experimental details.. .. .	6
3.2 Discussion of results	7
4. The Calculation of Corrections to the Overall Flow-rate in a Duct for the Effects of Pitot-stem Blockage	8
4.1 General	8
4.2 Blockage in a non-uniform velocity profile	8
4.3 Correction of local velocities measured in developed pipe-flow	11
4.4 Overall blockage corrections to the volume flow-rate measured in a circular pipe by the log-linear method ..	12
4.5 Overall blockage corrections to the volume flow-rate measured in a rectangular duct by the 26 point log-linear method	15

	<u>Page</u>
5. Conclusions	18
6. Acknowledgement	19
References	20
Figures 1 to 8	

1. List of Symbols

b	width or larger dimension of rectangular duct
C	cross-sectional area of pipe or duct
C_D	drag coefficient. Drag/qS
C_p	pressure coefficient. $(p - P)/q$
C_{P_b}	separation-pressure coefficient $(p_b - P)/q$
d	diameter of pitot stem
D	internal diameter of pipe
h	height or smaller dimension of rectangular duct
H	total-pressure
k	blockage factor for small values of S/C (Sect.3.2)
k'	measured blockage factor for large values of S/C
m	reciprocal of power-law index (Eqn.7)
n	factor representing velocity increment equivalent to blockage (Sect.4.2)
p	static-pressure of flow. Surface pressure at point on body in flow
p_b	surface pressure at separation point on body in flow
P	static (or surface) pressure in infinite stream
q	dynamic pressure $(H - p)$
Q	volume flow-rate
r	radial distance from axis of circular pipe

R	internal radius of circular pipe
$R_{D_{max}}$	pipe Reynold's number based on pipe diameter and velocity on axis $(U_{o_{max}} D/\nu)$
S	area of model chosen to define drag coefficient. Projected area normal to stream of exposed stem
U	velocity component parallel to longitudinal axis of pipe or duct
x	longitudinal distance from axis of stem (particularly to plane of static pressure holes),
z	exposed length of stem (measured from axis of head to wall of duct).
α	ratio $\left(\frac{z}{R}\right)\left(\frac{U_{o_{max}}^2}{U_o^2}\right)$ or $\left(\frac{z}{h}\right)\left(\frac{U_{o_{max}}^2}{U_o^2}\right)$ Eqns. 21, 24.
θ	Maskell's blockage constant $\left(-1/C_{P_{bc}}\right)$
ν	kinematic viscosity
ρ	fluid density
ϕ	ratio mean dynamic pressure over area of pipe to dynamic pressure on axis of pipe. Eqn. 13.
Suffix c	corrected for blockage (Maskell's notation)
Suffix max.	value on axis of pipe or duct
Suffix o	value in absence of stem
Suffix 1 to 7	value measured at position corresponding to that shown in Fig.7.

2. Introduction

Ower and Johansen¹ showed that the basic calibration factor of a pitot-static tube is governed by the relative distance between the plane of the static pressure holes and the axis of the cylindrical stem. In the absence of a stem, the pressure recorded by the static pressure holes is usually lower than the free stream static pressure. Retardation of the fluid as it approaches the stem causes the recorded static pressure to rise, so that by judicious positioning of the plane of the static pressure holes the basic calibration factor can be made equal to unity if so desired.

The pressure relationships which determine the basic calibration factor only apply in a fluid of infinite extent. If the tube is used in a finite duct, these pressure relationships are modified by the blockage effect as the fluid accelerates to pass the restricted passage in the plane of the stem. The static pressure recorded becomes less than the true value in the same plane with the tube removed.

The blockage error increases (a) as the plane of the static pressure holes approaches the axis of the stem and (b) as the ratio of the projected area of the stem normal to the flow, to the sectional area of the duct increases.

The author was not aware of any method by which these blockage corrections could be calculated except in the plane of the stem. It was therefore necessary to determine the magnitude of blockage corrections ahead of the stem by measurement in a wind tunnel.

Throughout the report the term "stem blockage" is intended to cover the blockage effect of the stem of

- (a) a static pressure tube on its own reading
- (b) a pitot-static tube on its static pressure reading
- (c) a total pressure (or pitot) tube on the reading of static pressure holes on the duct wall.

The resultant effect in each case is to overestimate the dynamic pressure measured at any point in the duct.

3. Measurement of the Blockage Effect due to a Stem of Circular Section

3.1 Experimental method

3.1(a) Basis of method

The method chosen was based on the author's previous experiments² connected with Maskell's theory for blockage effects on bluff models in a closed wind tunnel³.

From a study of thin flat plates normal to the wind, Maskell had derived an expression for the relationship between the measured pressure coefficient C_p at any point on a model and the corresponding value C_{p_c}

for the same point on a model in an infinite stream.

Maskell showed that

$$\frac{1 - C_p}{1 - C_{p_c}} = \frac{C_D}{C_{D_c}} = 1 + \theta C_D S/C \quad \dots(1)$$

where C_D is the measured separation-drag coefficient for the model, based on an area S , in a tunnel of cross-sectional area C , C_{D_c} is the

corresponding/

corresponding value in an infinite stream and θ is a non-dimensional blockage factor equal to $-(1/C_{p_{bc}})$, where $C_{p_{bc}}$ is the value of the pressure coefficient at the separation point on the model in an infinite stream.

For thin flat plates the separation-drag is equal to the measured drag. For relatively deep models enveloped in a separated wake from the leading edge Cowdrey⁴ has shown that equation (1) still applies as long as one takes C_D to be equal to the measured drag coefficient, increased to allow for buoyancy effects on the model within the wake (i.e., replacing the solid model by an equivalent model which terminates at the separation line). The present author confirmed² that the drag relationship given in equation (1) applied for plates and grids normal to the wind regardless of their position in the tunnel (e.g. mounted centrally or adjacent to a wall).

Furthermore, the attenuation of the blockage effect at stations ahead of the model depended on the ratio of the distance ahead of the model to the square-root of the area of the tunnel section. More explicitly, in the present context,

$$\frac{1 - C_{p_x}}{1 - C_{p_{xc}}} = 1 + \theta C_D \left(\frac{S}{C} \right) f \left(\frac{x}{\sqrt{C}} \right) \quad \dots(2)$$

where C_{p_x} is the static pressure coefficient measured at a distance x ahead of the model and on a chosen line parallel to the tunnel axis, $C_{p_{xc}}$ is the corresponding value in an infinite stream, $f(x/\sqrt{C})$ is an attenuation factor. The present author found that the same attenuation factor applied to both plates and grids normal to the flow.

In the present application we are concerned with small amounts of blockage associated with pitot tubes of sensible dimensions relative to the duct to be traversed. In these circumstances we may consider C_D in the product terms of equations (1), (2) to be constant, so that the blockage effect should be substantially linear with (S/C) . We may then consider the product (θC_D) as a single constant to be determined experimentally.

Earlier theoretical work by Glauert was extended by Thom⁵ to cover blockage due to general models including thick wings in a closed tunnel.

The method used assumed that the "solid blockage" effect due to the shape of the model was separable from the "wake blockage" effect due to the drag, and that these could be calculated separately and then combined. Thom showed that the pressure change at the wall due to solid

blockage was greater than that on the tunnel axis, for any plane ahead of a model. However, the pressure changes due to wake blockage were constant across any such plane.

It is now generally accepted that the flow around bluff bodies cannot be separated into inviscid and viscous components, because the presence of each affects the other. This is emphasised by the fact that Thom's values for the wake blockage factor θ were much too low. However, Thom's treatment did suggest there were physical reasons for suspecting that the blockage effect ahead of bluff models of finite volume might not be constant across any transverse plane. Moreover Thom's work showed the advisability of measurement of the unconstrained pressure distribution ahead of a finite wall-mounted cylinder when this was required in the present investigation, rather than reliance on calculation.

3.1(b) Experimental details

The measurements were made in two wind tunnels. One had a closed working section 16.8 ins \times 28.8 ins (0.427 m \times 0.732 m) with fillets at each corner to give a sectional area at the model 3.25 ft² (0.35 m²). The other was an open-jet tunnel with an elliptical jet 9 ft \times 7 ft (2.74 m \times 2.13 m) with a sectional area 49.5 ft² (5.33 m²). Both by virtue of its large area and by the fact that it had an open working section, the second tunnel could be considered almost free from blockage effects on a given model in comparison with the former tunnel.

The model chosen to represent the stem of a pitot tube was a brass cylinder 3 ins (0.076 m) in diameter, and 22 ins (0.558 m) long, terminated in a hemispherical cap at one end, the other end being plane. A more realistic model would have been impractical because of the need to traverse just ahead of the stem. The model fitted a flanged collar screwed to the outside of the tunnel so that the model could be inserted to any required depth or retracted and reversed to present a flush surface at the wall. The arrangement is shown in Fig.1.

A wall reference static pressure tapping was fitted 67 ins (1.7 m) ahead of the model. A very small static pressure tube was used for the main measurements and a Bradshaw micromanometer⁶ was connected between this and the reference tapping. All static pressure measurements were made in the vertical central plane of the working section. One set was made on the centre line of the tunnel ahead of the model, another set at 2½ ins (0.064 m) from the floor (i.e. very close to the floor but outside the influence of turbulence from the floor boundary layer). In the centre line position the static pressure tube was inserted from the side wall to reduce the insertion length and thus minimise tube vibration.

The tunnel speed was deliberately limited to about 90 ft/s (27.4 m/s) for all measurements so that the Reynolds number based on stem diameter did not exceed 1.5×10^5 (below the limit of the sub-critical constant drag coefficient range). In consequence the drag coefficient of the model should have been very close to that of a typical pitot tube stem used at low speeds.

Measurements were made in the closed wind tunnel at several planes ahead of the model. Each measurement recorded the change in static pressure between the empty tunnel condition and that with the cylinder inserted to a given depth. Several insertion depths were used to check the dependence on S/C.

Measurements were repeated in the open jet tunnel with the cylinder mounted on a ground board in the flow. The reference static pressure tube for these measurements was placed well ahead of the model position on the diametrically opposite side of the jet.

From such pairs of measurements, the blockage-free pressure difference, due to the presence of the model, was subtracted from the total measured pressure difference in the closed tunnel, to give the pressure difference due to blockage alone.

3.2 Discussion of results

Individual graphs of the pressure difference due to blockage plotted against the insertion parameter (S/C) followed a linear relationship of the form

$$\Delta C_p = -k' (S/C) \quad \dots(3)$$

where k' was a function of (x/\sqrt{C}) . This was anticipated in Section 2(a).

Measurements on the centre-line were abandoned for the range $d/2 < x < 5d/2$, (i.e. 2 diameters ahead of the model) because of the extreme sensitivity of the measured static pressure in this range to positional and directional errors. Outside this range the centre-line values of k' were consistently 13% less than those close to the wall. This was qualitatively what Thom⁴ had predicted; numerically the measured values of k' were greater than those calculated from his formulae. It was possible to deduce a plausible value $k' = 1.04$ for the centre-line value at $x = 0$ by assuming the 13% difference between wall and centre-line positions persisted up to the model.

The model had been originally chosen to be large (S/C at full insertion = 0.103) to produce conveniently large pressure changes for measurement. A more usual value of S/C for a pitot tube in accurate pipe flow measurements would be 0.02, or at the most 0.05. Thus the use of a large model had resulted in an unrepresentative increase in the value of C_D for the model by a factor $[1 + 1.04 (S/C - 0.02)]$ or 1.087 at full insertion. Since the parameter k' includes the product θC_D , all values of k' were reduced by this factor to yield values k more relevant to practical values of (S/C). Values of k are shown in Fig.2.

For a wall-mounted finite cylinder at sub-critical Reynolds numbers $C_{p_{D0}}$ would be about - 0.8, so that the reciprocal, of reversed sign, θ should be about 1.25. An average value of C_D for this model

might/

might be 0.9 making k at $x = 0 (= \theta C_D)$ about 1.1. This compares well with the measured values. However, as Maskell has pointed out³, in some Reynolds number ranges blockage might well affect the separation position and in consequence the separation pressure coefficient on a cylinder. It would be inadvisable to assume that there will always be good agreement between infinite stream measured values of $(-1/C_{p_{bo}})$ and θ at higher Reynolds

numbers. In the present application the magnitude of the static pressure correction for stem blockage would normally be small, so that differences between corrections on the axis of the duct and those on the wall may be ignored. Then an average curve for K (as in Fig.3) could be used both for combined pitot-static tubes and for pitot tubes used in conjunction with a wall static pressure tapping.

4. The Calculation of Corrections to Overall Flow-rate in a Duct for the Effects of Pitot-stem Blockage

4.1 General

From the main report it follows that the presence of a pitot-stem in a duct with uniform flow requires the measured values of local dynamic pressure to be reduced by an amount,

$$\Delta q = k(S/C) \quad \dots(5)$$

For accurate flow measurement in ducts it is also necessary to ensure that the turbulence is not unduly high and to correct for it. These requirements are best met by making flow measurements in long smooth circular pipes where the turbulence characteristics are reproducible, moderate and known. In such fully developed pipe flow the mean-velocity profiles are stable and depend only on pipe Reynolds number, so that measurements at a few radial positions, chosen by the log-linear method⁷, will suffice to give an accurate mean flow velocity. Once the number of points of measurement per diameter have been chosen the location of the measuring positions follows automatically.

In these circumstances it is convenient to calculate the effect of corrections for blockage (and other effects) at each point of measurement and to assess the overall effect of neglecting such corrections on individual readings with the intention of applying overall corrections to the volume flow rate.

An essential preliminary step in such calculations is the assessment of the effect of the non-uniform velocity profile in developed pipe flow on stem blockage.

4.2 Blockage in a non-uniform velocity profile

Maskell's theoretical treatment of blockage corrections for bluff bodies in closed wind tunnels is based on the assumption of a uniform velocity profile far ahead of the model. The measurements described earlier in this paper were made under similar uniform velocity conditions. A formal analysis for non-uniform velocity conditions would probably prove too

difficult/

difficult and so one has to rely on known basic features of blockage and bluff-body aerodynamics in order to apply the uniform flow pitot-stem corrections to the more general developed pipe flow case.

From measurements of the base pressure on flat plates normal to the wind in a closed wind tunnel, Maskell was able to confirm assumptions in his theory that blockage effects on bluff bodies in a closed wind tunnel were equivalent to an increase in the approach velocity, with the result that all velocities in the flow field outside the wake increase by the same factor.

The present author showed experimentally that the total blockage effect due to two flat plate or grid models in the same plane was the same as if the individual quantities $(\theta C_D S/C)$ were introduced by a single model representing the same total value of $(\theta C_D S/C)$.

Both of these features are consistent with the concept that the total effect of the infinite series of images of a model in any one tunnel wall is equivalent to a single concentrated image at a distance large compared with the dimensions of the working section, so that the blockage velocities induced by the single image are fairly constant over any given plane of the working section, irrespective of the position of the model or models in their common plane.

Fig.4 shows measured values of the ratio $(-C_D/C_{p_b})$ measured on a floor mounted cylindrical model (length/diameter = 12) in conditions of negligible blockage and sub-critical Reynolds numbers with a uniform approach velocity profile and also with a non-uniform power-law profile of index 1/5. The measurements were incidental to an investigation of wind-loading on chimneys including surface flow visualisation, so that the boundary layer separation position at any height was known and there was no difficulty in deciding the circumferential position at which the surface pressure was equal to C_{p_b} .

It will be seen that, for present purposes at least, the values of $-(C_D/C_{p_b})$ are not seriously affected by the velocity gradient in the non-uniform flow, since the velocity profiles found in developed pipe flow are intermediate between the profiles tested. On this evidence one may conclude that each small cylindrical element which constitutes the whole cylinder will contribute the same value $\Delta(\theta C_D S/C)$ in a non-uniform stream as in uniform flow. It follows that the blockage effect, as defined by the factor $(1 + n)$, by which all velocities outside the wake are increased, will also remain unchanged whether the flow is uniform or not, and all values of local dynamic pressure will increase by approximately $(1 + 2n)$ when n is sufficiently small for n^2 to be neglected.

By comparison with equation (1) in Section 2.2(a)

$$2n = \theta C_D S/C$$

or/

or in terms of the experimental constant k,

$$2n = k S/C \quad \dots(6)$$

where values of k are plotted Fig.4.

The approach velocity profile in the pipe may be expressed in the power-law form for fully-developed flow,

$$\frac{U_o}{U_o \max} = \left(1 - \frac{r}{R}\right)^{\frac{1}{m}} \quad \dots(7)$$

where the local approach velocity is U_o at a radius r , $U_{o \max}$ on the pipe axis, R the pipe radius and m is a constant depending on the Reynolds number of the flow.

The corresponding ratio of the dynamic pressures will be

$$\frac{q_o}{q_o \max} = \left(1 - \frac{r}{R}\right)^{\frac{2}{m}} \quad \dots(8)$$

In a circular pipe, mean values of these ratios will be

$$\frac{\bar{U}_o}{U_o \max} = \frac{2m^2}{(m+1)(2m+1)} \quad \dots(9)$$

and

$$\frac{\bar{q}_o}{q_o \max} = \frac{m^2}{(m+2)(m+1)} \quad \dots(10)$$

If all velocities in the power-law profile are increased by a factor $(1+n)$ these ratios are unchanged. We may therefore apply Bernoulli's equation to the mean values of the dynamic pressure in a pipe with and without blockage to find the change in static pressure caused by blockage.

Thus,

$$\bar{H} = p_o + \bar{q}_o = p + (1+2n)\bar{q}_o \quad \dots(11)$$

so that

$$\Delta C_{p_o} = (p - p_o)/\bar{q}_o = -2n = -k S/C \quad \dots(12)$$

In terms of the axial value of the dynamic pressure,

$$\Delta C_{p_o \max} = (p - p_o) / q_{o \max} = -(k S/C) (\bar{q}_o / q_{o \max}) = -\phi k S/C \quad \dots(13)$$

Since blockage corrections will normally be small, there is no need to obtain $(\bar{q}_o / q_{o \max})$ for a circular pipe by integration of experimental results. Fig. 5 shows values of this parameter ϕ for a range of pipe Reynolds numbers (based on the axial velocity $U_{o \max}$). These values have been obtained from equation (10) using accepted values of m for fully developed flow in smooth pipes.

4.3 Correction of local velocities measured in developed pipe flow

It is usual to express local velocities, measured in a circular pipe, as fractions of the axial velocity, so that any subsequent integration process is non-dimensional. The stem-blockage corrections for this purpose are best made in two stages. The axial dynamic pressure reading is first corrected; that is

$$q_{o \max} = q_{\max} [1 - \phi k S/C] \quad \dots(14)$$

where S/C for this reading has the value $\frac{2}{\pi} \left(\frac{d}{D} \right)$.

Then the readings of local dynamic pressure are made non-dimensional in terms of the corrected value $q_{o \max}$. These are subsequently corrected according to equation (13) whereby

$$\left(\frac{q_o}{q_{o \max}} \right) = \left(\frac{q}{q_{\max}} \right) - \phi k S/C = \left(\frac{U_o}{U_{o \max}} \right)^2 \quad \dots(15)$$

The derived values of $U_o / U_{o \max}$ are available for graphical integration.

It is possible to correct in one stage by means of a single equation, but the arithmetic is less simple. The single equation is

$$\frac{U_o}{U_{o \max}} = \left[1 + \frac{\phi k}{\pi} \left(\frac{d}{D} \right) - \frac{\phi k}{2} \left(\frac{S}{C} \right) \left(\frac{q_{\max}}{q} \right) \right] \sqrt{\frac{q}{q_{\max}}} \quad \dots(16)$$

where the neglect of higher order terms in the expansion has a negligible effect in the context of normal flow measurement.

From the individual corrected measurements of $U_o / U_{o \max}$, graphical
integration/

integration is normally used to derive a mean value $\bar{U}/U_{o\max}$ for the section traversed. The corrected flow rate then becomes

$$Q_o = C \left(\frac{\bar{U}_o}{U_{o\max}} \right) \sqrt{\left(\frac{2q_{o\max}}{\rho} \right)} \quad \dots(17)$$

Similarly a single corrected velocity would be

$$U_o = \left(\frac{U_o}{U_{o\max}} \right) \sqrt{\left(\frac{2q_{o\max}}{\rho} \right)} \quad \dots(18)$$

Such point by point correction is tedious. Traversing methods based on fixed points of measurement (such as the log linear method) are much to be preferred because it is possible to make a single overall correction to the flow rate calculated from uncorrected individual readings. This is discussed in the next section.

4.4 Overall blockage corrections to the volume flow-rate measured in a circular pipe by the log-linear method

It is possible to calculate corrections to the overall flow-rate in fully developed pipeflow, for general application at a particular Reynolds number, provided traverses are made on each diameter by means of measurements at fixed radial positions. Such corrections are applied finally to flow-rates which have been estimated from uncorrected readings. If we convert equation (13) into the approximate form

$$\left(\frac{U_o}{U_{o\max}} \right) = \left(\frac{U}{U_{o\max}} \right) \left[1 - \frac{1}{2} \phi k \left(\frac{S}{C} \right) \left(\frac{q_{o\max}}{q_o} \right) \right] \quad \dots(19)$$

the error in substituting $(q_{o\max}/q_o)$ for $(q_{o\max}/q)$ in the correction term will be negligible in the present application.

For the measurement of flow-rate in a pipe we require corrected values U_o [i.e. $(U_o/U_{o\max})U_{o\max}$]; whereas the stem-blockage error would arise from the use of uncorrected values U [i.e. $(U/U_{o\max})U_{o\max}$]. Thus we can assess the errors due to blockage by consideration of the difference between the terms $U_o/U_{o\max}$ and $U/U_{o\max}$ at each point of measurement.

From (19) it follows that

$$\left(\frac{U_o}{U_{o\max}} \right) = \left(\frac{U}{U_{o\max}} \right) \left[1 - \frac{1}{2} \phi k \left(\frac{S}{C} \right) \left(\frac{U_{o\max}^2}{U_o^2} \right) \right] \quad \dots(20)$$

Thus/

Thus the error

$$\Delta \left(\frac{U}{U_{\max}} \right) = -\frac{1}{2} \phi k \left(\frac{S}{C} \right) \left(\frac{U_o^2}{U_o^2} \right)$$

If D is the pipe diameter (= 2R), d the pitot-stem diameter and z the immersion depth of the stem in the fluid we may write

$$\left(\frac{S}{C} \right) = \left(\frac{z}{R} \right) \left(\frac{d}{D} \right) \left(\frac{2}{\pi} \right) \text{ so that the error may be written more}$$

conveniently for calculation as

$$\Delta \left(\frac{U}{U_{\max}} \right) = - \left(\frac{1}{\pi} \right) \left(\frac{d}{D} \right) \phi k \left[\left(\frac{z}{R} \right) \left(\frac{U_o^2}{U_o^2} \right) \right] \dots(21)$$

The product in the square bracket varies for each position of measurement and the mean value of this product for all points of measurement is evaluated first, then multiplied by the other product to derive the overall error on volume flow-rate.

We will consider as an example measurements of airflow through an 18 in (0.457 m) diameter pipe with an axial velocity of about 80 ft/s (24.4 m/s). The measurements would be made at either 10 or 6 points per diameter at radial positions derived from general expressions for the log linear method given by Winternitz and Fischl⁷. This method yields average flow velocities on each diameter traversed, by taking the arithmetical mean of the velocities measured at each radial position. An extra measurement is required on the axis of the pipe solely for blockage correction. We will consider the measurements to be made in alternative ways, (a) with a single insertion hole per diameter, so that the pitot-stem immersion can exceed one radius for some readings and (b) with two insertion holes per diameter so that the pitot-stem immersion never exceeds one radius. For the example chosen the pipe Reynolds number

$R_{D \max} (= U_{o \max} D/\nu) \approx 0.75 \times 10^6$ and in fully developed pipe flow the velocity profile may be expressed in the form

$$\left(\frac{U_o}{U_o \max} \right) = \left(1 - \frac{r}{R} \right)^{1/0.5}$$

The calculations are set out below to demonstrate the relative contributions to the blockage error at the various measurement stations, as indicated by the magnitude of the product term.

10 point log-linear method

Full diameter insertion

	One radius insertion									
$\frac{z}{R}$.038	.152	.306	.434	.722	1.278	1.566	1.694	1.848	1.962
$\frac{U_o}{U_o \text{ max}}$.707	.821	.883	.916	.966	.966	.916	.883	.821	.707
$\left(\frac{z}{R}\right) \left(\frac{U_o \text{ max}}{U_o}\right)^2$.076	.225	.393	.517	.733	1.370	1.865	2.087	2.740	3.930

Mean of first 5 points = 0.397

Mean of 10 points = 1.398

6 point log-linear method

Full diameter insertion

	One radius insertion					
$\frac{z}{R}$.064	.270	.642	1.358	1.730	1.936
$\frac{U_o}{U_o \text{ max}}$.749	.871	.955	.955	.871	.749
$\left(\frac{z}{R}\right) \left(\frac{U_o \text{ max}}{U_o}\right)^2$.114	.356	.705	1.490	2.277	3.450

Mean of first 3 points = 0.392

Mean of 6 points = 1.399

These figures show that the stem blockage errors are virtually identical whether the 6 point or 10 point per diameter method is used for the velocity profile typical of this Reynolds number range.

If we let the mean value of $(z/R) \left(\frac{U_o \text{ max}}{U_o}\right)^2$ equal $\bar{\alpha}$ then at $R_{D \text{ max}} = 0.75 \times 10^6$ $\bar{\alpha} = 0.395$ or 1.398 for one-radius insertion and one-diameter insertion respectively.

Inserting these values in equation (21) with the corresponding values for ϕ we have for $R_{D \text{ max}} = 0.75 \times 10^6$

$$\frac{\Delta Q}{Q}$$

$$\left. \begin{aligned} \frac{\Delta Q}{Q} &= - .093 k \left(\frac{d}{D} \right) && \text{for two insertion holes per diameter} \\ \frac{\Delta Q}{Q} &= - .332 k \left(\frac{d}{D} \right) && \text{for a single insertion hole per diameter} \end{aligned} \right\} (22)$$

If we repeat these calculations for $M = 6$ corresponding to a Reynolds number $R_{D \max} = 1.7 \times 10^4$ (which represents the approximate lower limit for accurate flow measurement) we find that

$$\left. \begin{aligned} \frac{\Delta Q}{Q} &= - .091 k \left(\frac{d}{D} \right) && \text{for two insertion holes per diameter} \\ \frac{\Delta Q}{Q} &= - .359 k \left(\frac{d}{D} \right) && \text{for a single insertion hole per diameter} \end{aligned} \right\} (23)$$

The small scale effect resulting from this large change in Reynolds number is insignificant in the calculation of blockage corrections and it is suggested that the values for $R_{D \max} = 0.75 \times 10^8$ should be applied to all flow measurements in pipes.

Values of k have been inserted in equations (22) for pitot-static tubes of various stem/pipe diameter ratios (d/D) and with stem to static hole distances $x = 0, 8d$ and $16d$. The value $x = 0$ applies to the cantilever pitot-tube; $x = 8d$ corresponds to the most-used range of pitot-static tubes; $x = 16d$ represents a pitot-static tube with a generously long head. Each set applies equally to the case of a pitot-tube used with pipe-wall static pressure tappings where the stem of the pitot tube is in a plane at a distance x from the plane of the wall tappings.

The results are plotted in Fig.6. The benefit of the use of two insertion holes per diameter in the reduction of blockage corrections is clearly shown. The advantage of longer pitot-static tubes in this respect can also be seen. Other values of x/d may be considered by taking the appropriate values of k according to the values x/\sqrt{C} from Fig.3. For considering a whole range of conditions it is useful to evaluate x/\sqrt{C} for a circular pipe as $(2/\sqrt{\pi})(x/d)(d/D)$.

4.5 Overall blockage corrections to the volume flow-rate measured in a rectangular duct by the 26 point log-linear method

Information on fully developed flow in rectangular ducts is less complete than that for circular pipes. Nevertheless there is sufficient information to make an estimate of overall corrections to the volume flow-rate for methods which use fixed measuring points. The most promising of such methods is the 26 point log-linear method. Myles, Whittaker and Jones⁸ give details of velocity traverses made in square and duplex ducts in order to check the performance of the 26 point method.

The traverses need to be made along four lines parallel to one edge (the shorter, if the duct is not square), and the traverse positions are shown in Fig.7.

We will consider a quarter duct with 7 points of measurement. The mean velocity through a quarter duct is given by

$$\bar{U} = 1/24 \left[2 (U_1 + U_2 + U_3) + 3 (U_3 + U_4 + U_5 + U_6) + 6U_7 \right] \dots(23)$$

where U_n is the local velocity at a point n in Fig.7. Myles et al⁸ give measured values of the velocity at each point and of \bar{U} in terms of U_{max} , the velocity on the axis of the complete duct.

Once again the error on each local reading due to stem blockage follows from equation (20)

$$\Delta \left(\frac{U}{U_{max}} \right) = \frac{1}{2} \phi k \left(\frac{S}{C} \right) \left(\frac{U_o^2}{U_o^2} \right)$$

For the rectangular duct, with stem insertions parallel to the shorter side, this becomes

$$\Delta \left(\frac{U}{U_{max}} \right) = \frac{1}{2} \phi k \left(\frac{d}{b} \right) \left[\left(\frac{z}{h} \right) \left(\frac{U_o^2}{U_o^2} \right) \right]$$

and according to N.E.L. Report 251, $\phi = (0.845)^2 = 0.714$

Thus

$$\Delta \left(\frac{U}{U_{max}} \right) = 0.357 k \left(\frac{d}{b} \right) \left[\left(\frac{z}{h} \right) \left(\frac{U_o^2}{U_o^2} \right) \right] \dots(24)$$

As for the circular duct, we will find the effective mean value of the terms

$\alpha = (z/h)(U_o^2/U_o^2_{max})$ first. This is given by

$$\bar{\alpha} = 1/24 \left[2 (\alpha_1 + \alpha_2 + \alpha_3) + 3 (\alpha_3 + \alpha_4 + \alpha_5 + \alpha_6) + 6\alpha_7 \right]$$

We will assume the pitot tube to be inserted from the top of the duct when only one insertion hole per diameter is used.

Upper quarter-duct

<u>Point</u>	<u>(z/h)</u>	<u>(U_o/U_{o max})</u>	<u>α</u>
1	.034	.708	0.068
2	.092	.796	0.145
3	.250	.807	0.384
4	.500	.815	0.753
5	.034	.715	0.067
6	.250	.952	0.276
7	.367 _s	.988	0.377

Lower quarter-duct

<u>Point</u>	<u>(z/h)</u>	<u>(U_o/U_{o max})</u>	<u>α</u>
1	.966	.708	1.928
2	.908	.796	1.433
3	.750	.807	1.151
4	.500	.815	0.753
5	.966	.715	1.890
6	.750	.952	0.828
7	.632 _s	.988	0.648

$\bar{\alpha}$ for the upper section only = 0.329
 $\bar{\alpha}$ for both sections = 0.723

The error on the overall measured flow-rate follows from equation (24),

$$\frac{\Delta Q}{Q} = 0.357 \bar{\alpha} k \left(\frac{d}{b} \right) \quad \text{so that}$$

$$\frac{\Delta Q}{Q} = 0.117 k \left(\frac{d}{b} \right) \quad \text{for two insertion holes per line of traverse}$$

$$\text{and } \frac{\Delta Q}{Q} = 0.258 k \left(\frac{d}{b} \right) \quad \text{for a single insertion hole per line of traverse.}$$

Values of k may be obtained for appropriate values of x/\sqrt{C} from Fig.3. A range of conditions may be covered more easily by evaluating x/\sqrt{C} as $(x/d)(a/b)\sqrt{(b/h)}$. Values of the overall correction have been calculated for

tubes/

tubes with a popular head-length characterised by $x = 8d$, for a range of values of d/b and with single or double insertion holes per line of traverse.

The results are shown in Fig.8 and once more show the increase in blockage correction which is necessary with a single insertion hole per line of traverse.

In the absence of information on scale effects on the velocity profiles in the N.E.L. measurements, one can only be guided by the circular pipe results and assume that the blockage corrections will not vary significantly over the range of Reynolds numbers covering practical flow measurements with pitot-tubes.

5. Conclusions

Measurements in uniform flow conditions in a duct have shown that the reduction in static pressure due to blockage by a cylindrical stem is constant across any particular plane ahead of the stem. The correction to the measured velocity at any point is thus the same whether the static pressure is measured by static or pitot-static tube associated with the stem, or by wall static pressure holes in the same plane in the presence of the stem of a total pressure tube.

The static pressure error is given by $\Delta C_p = -k S/C$ where k varies with the ratio of the distance between the axis of the stem and the plane of the static holes to the square root of the duct area, as shown in Fig.3.

In non-uniform flow it is shown that the corresponding error in any plane of measurement can be expressed as a change in the average dynamic pressure over the area of the plane of measurement

$$\Delta C_{p_o} = -k S/C$$

or as a change in the axial dynamic pressure

$$\Delta C_{p_o \text{ max}} = -\phi k S/C$$

where ϕ is the ratio of the average dynamic pressure to the axial value, shown for fully developed flow in circular pipes in Fig.5.

From this it follows that the corrected value of the ratio of a local velocity to the axial velocity on the same plane is related to the corresponding measured values of dynamic pressure by the equation

$$\frac{U_o}{U_o \text{ max}} \simeq \left[1 + \frac{\phi k}{\pi} \left(\frac{d}{D} \right) - \frac{\phi k}{2} \left(\frac{S}{C} \right) \left(\frac{q_{\text{max}}}{q} \right) \right] \sqrt{\frac{q}{q_{\text{max}}}}$$

Finally calculations are made for an overall single blockage correction to the flow rate through circular pipes and rectangular ducts subject to fully developed pipe flow, for correction of the flow rate calculated from uncorrected measurements of dynamic pressure according to

the/

the log linear method. The corrections are presented in Figs.6,8.

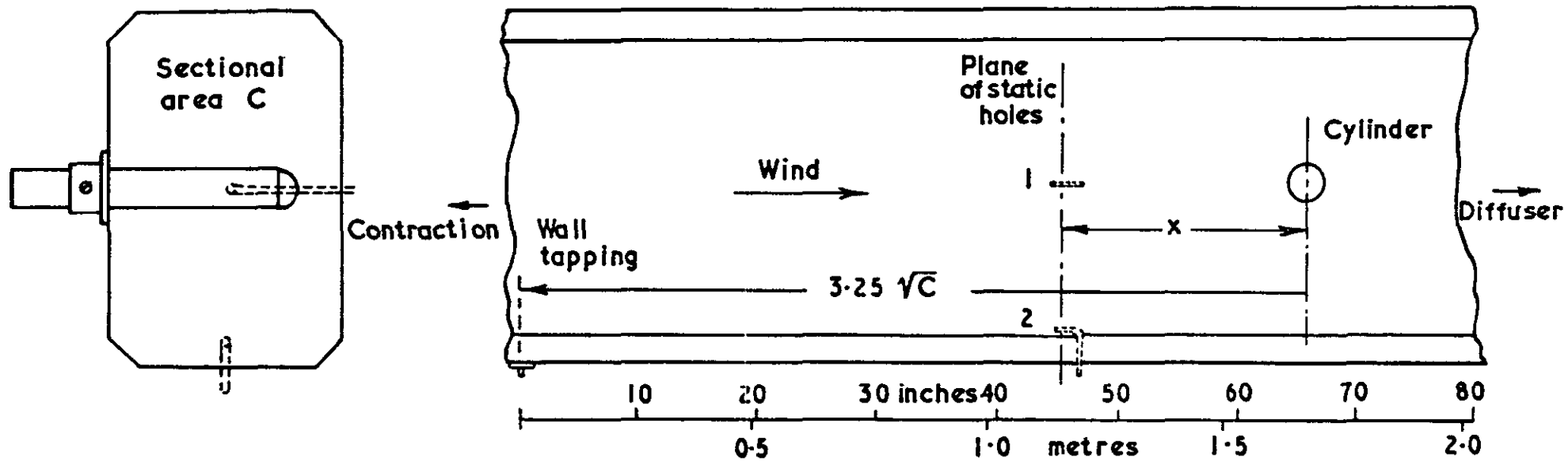
These calculations show that stem-blockage corrections will normally be small provided traverses are made from each wall to the centre of the duct, rather than from wall to wall.

6. Acknowledgement

Mr. W. G. Raymer made the wind tunnel measurements described in this report.

References

<u>No.</u>	<u>Author(s)</u>	<u>Title, etc.</u>
1	E. Ower and F. C. Johansen	The design of pitot-static tubes. ARC R & M 981 (1925).
2	R. W. F. Gould	Wake blockage corrections in a closed wind tunnel for one or two floor-mounted models subject to separated flow. A.R.C. R & M 3649.
3	E. C. Maskell	A theory for the blockage effect on bluff bodies and stalled wings in a closed wind tunnel. ARC R & M 3400 (1963).
4	C. F. Cowdrey	The application of Maskell's theory of wind-tunnel blockage to very large solid models. NPL Aero Report 1247 (1967).
5	A. Thom	Blockage corrections in a closed high speed tunnel. ARC R & M 2033 (1943).
6	P. Bradshaw	A compact null-reading U-tube micromanometer with an entirely-rigid liquid container. J. Scient. Instrum. 42 (1965) 677.
7	F. A. L. Winternitz and C. F. Fischl	A simplified integration technique for pipe-flow measurement. Water Power 9 (1957) 225.
8	D. J. Myles, J. Whittaker and M. R. Jones	A simplified integration technique for measuring volume flow in rectangular ducts. NEL Report No.251 (1966).



Arrangement for blockage measurements in a closed wind tunnel

FIG. 1

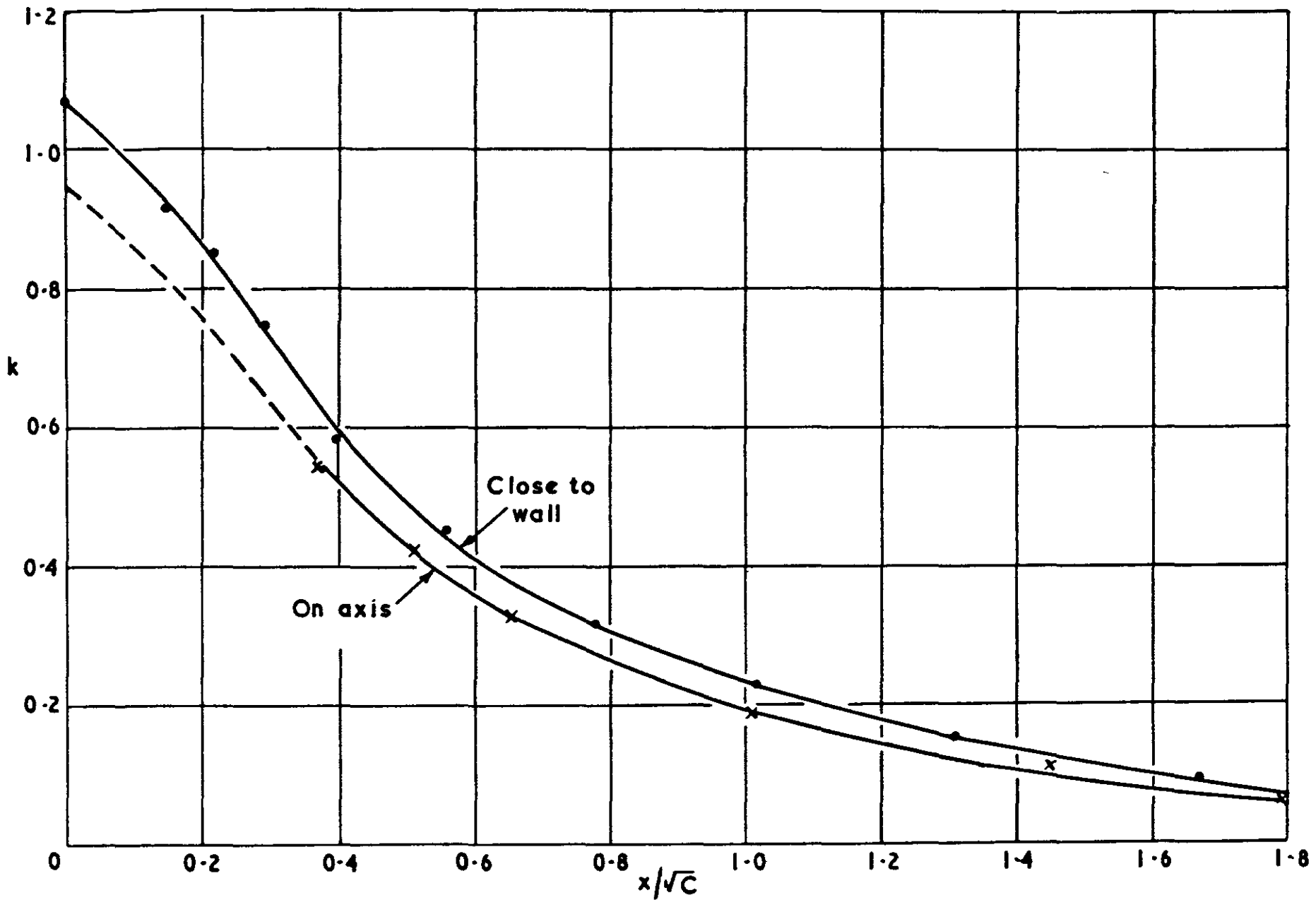
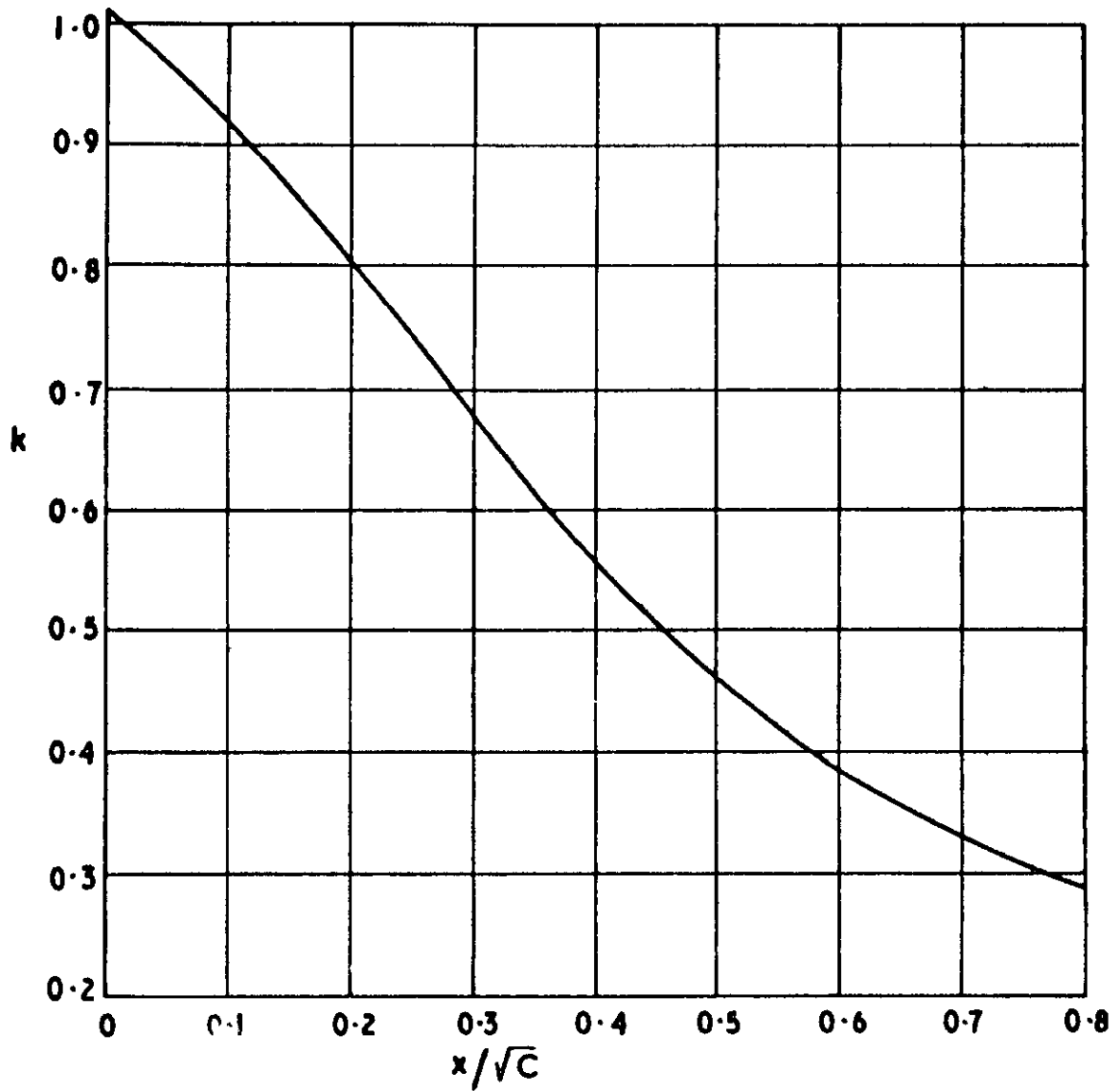


FIG. 2

Blockage constants for cylindrical stem of pitot-static tube affecting static pressure
measured (a) at tube (b) at wall static tapping

FIG. 3



Average value of blockage constant for cylindrical stem
of pitot-static tube for whole of any transverse plane

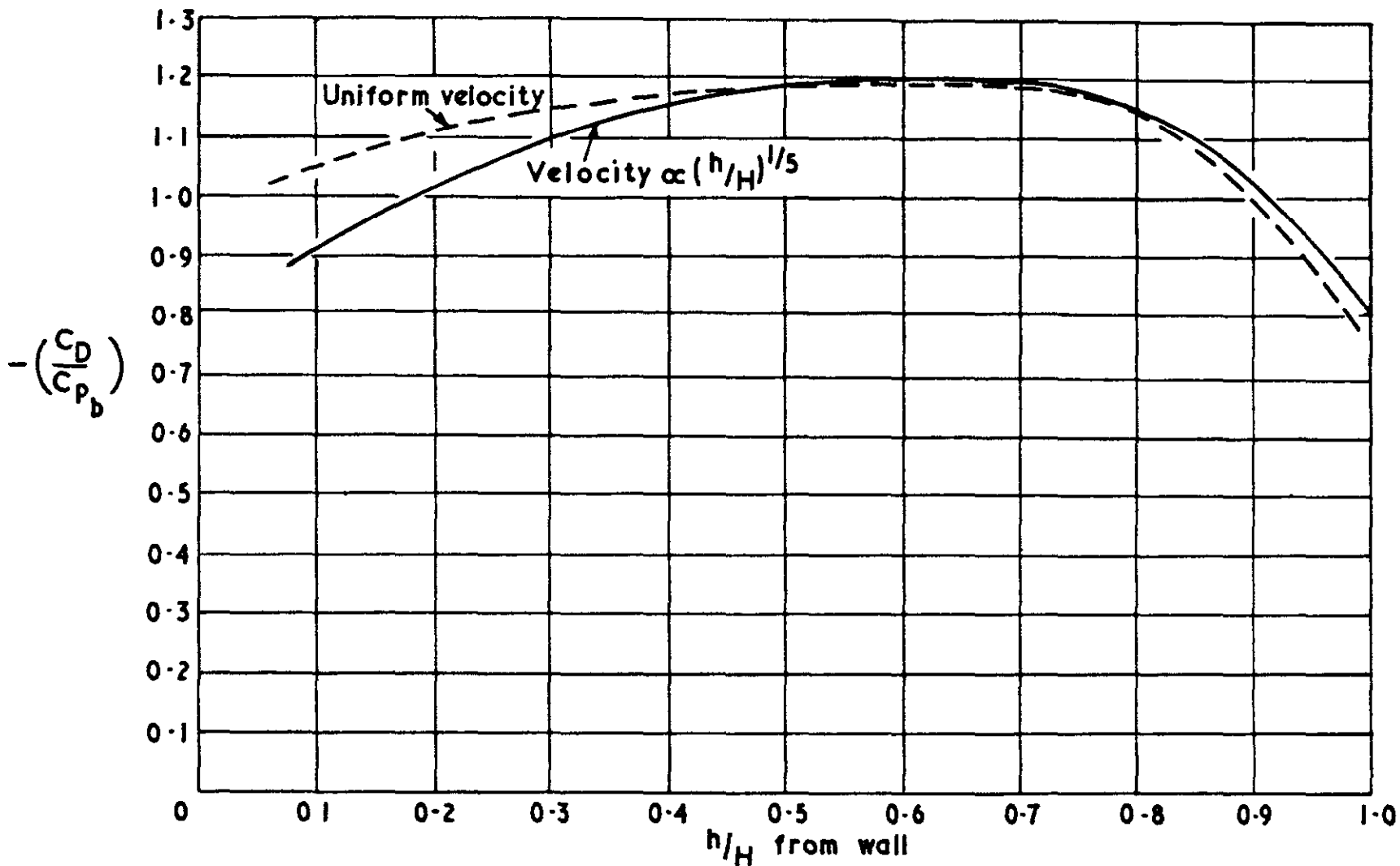
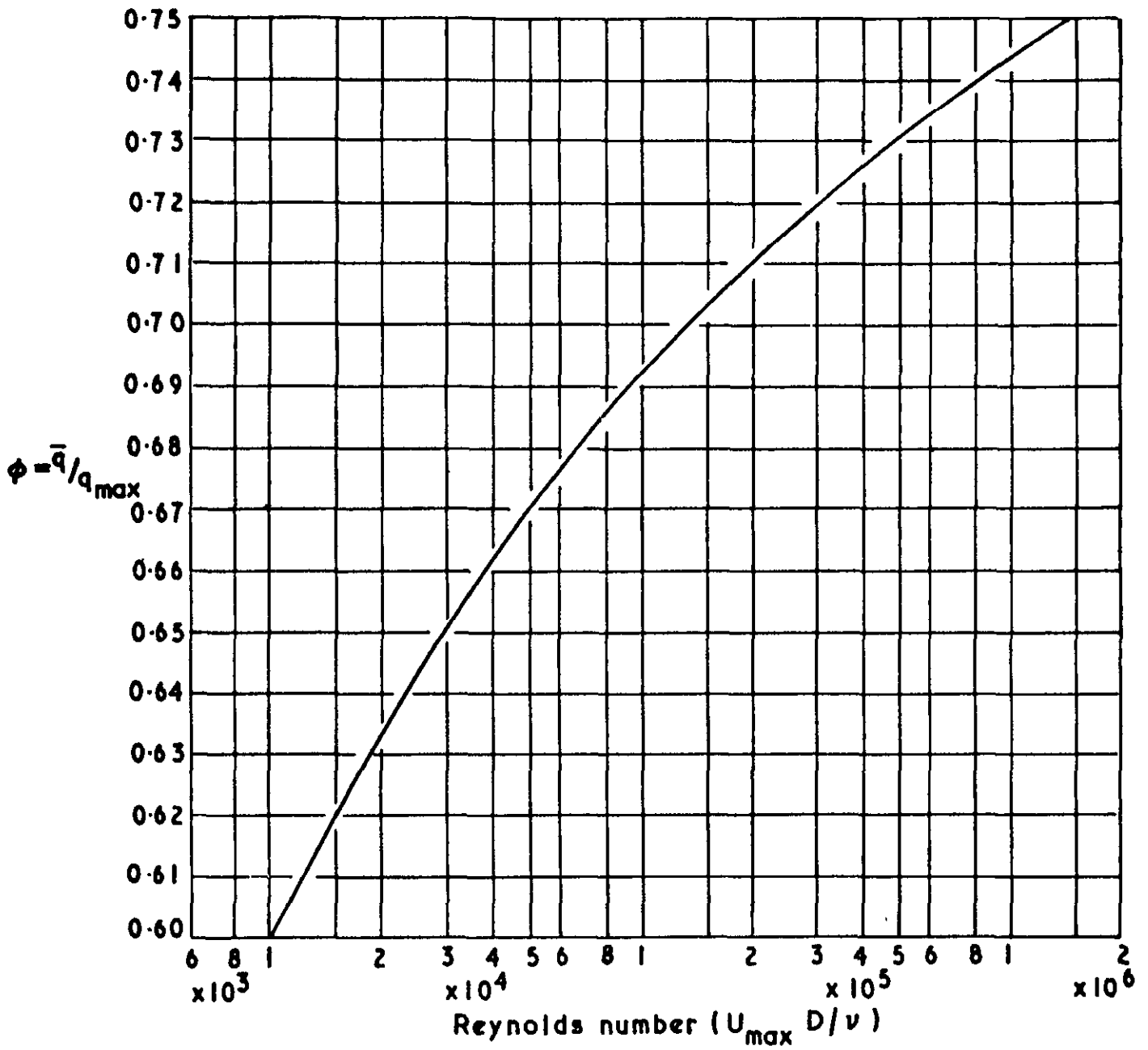


FIG.4

Values of $-(C_D / C_p)$ along length of cylinder of height $H=12$ diameters, normal to wall, in uniform flow and in a $1/5$ th power-law velocity profile, at

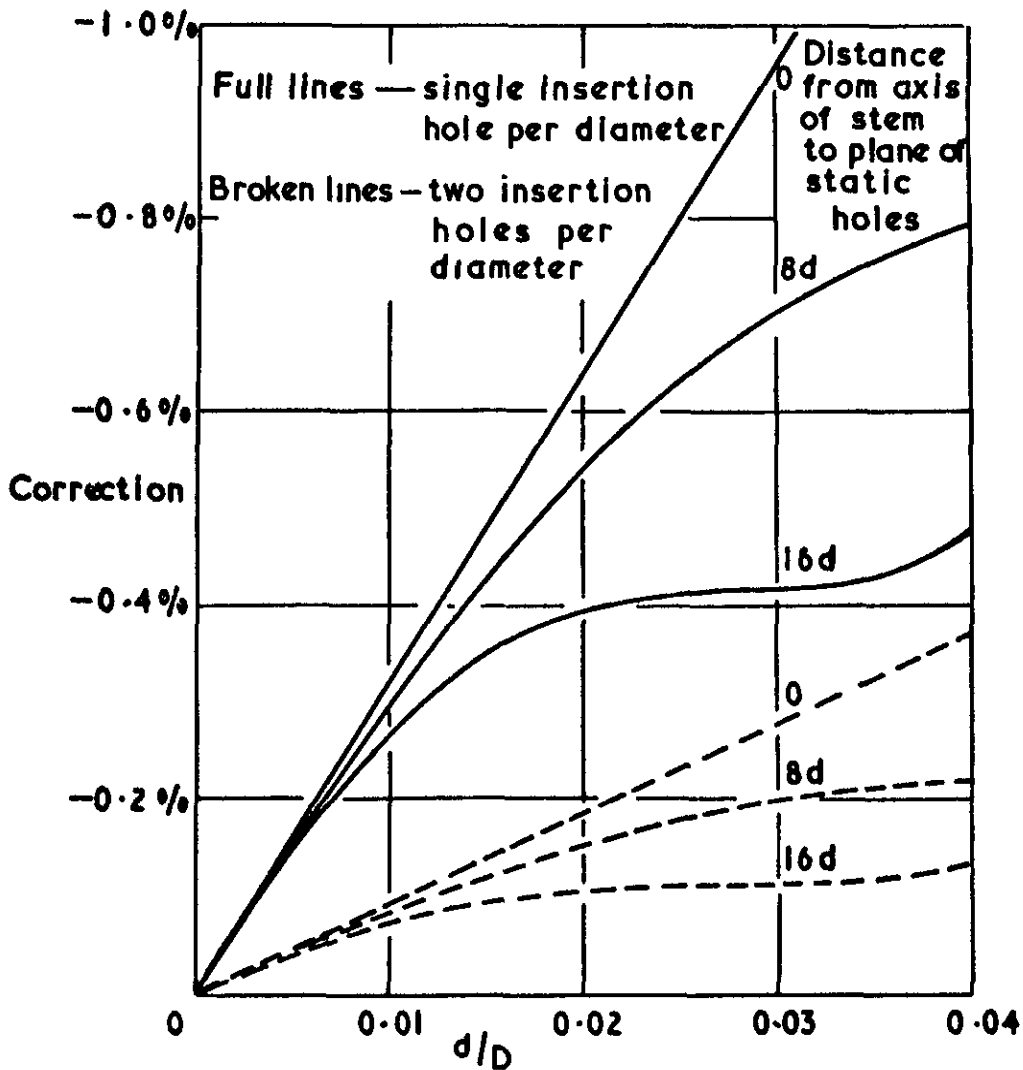
Reynolds numbers $\Delta 5 \times 10^4$

FIG. 5



Ratio of mean dynamic pressure to axial dynamic pressure in smooth circular pipes subject to fully developed flow

FIG.6



Pitot-stem blockage corrections to volume flow rate measured in smooth circular pipes by the log-linear method (6 or 10 points per diameter)

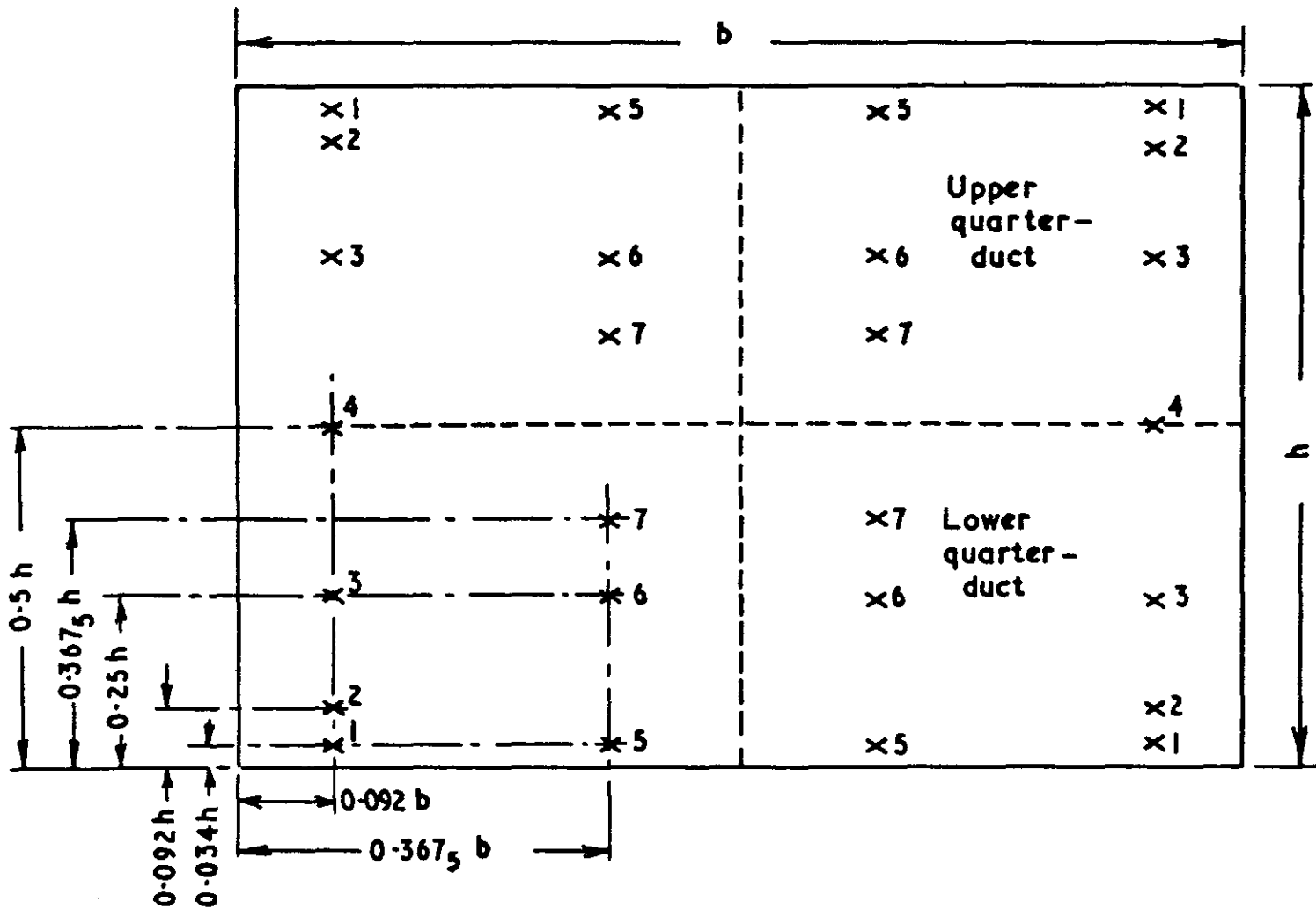


FIG. 7

Measurement positions for 26 point log-linear method in rectangular duct

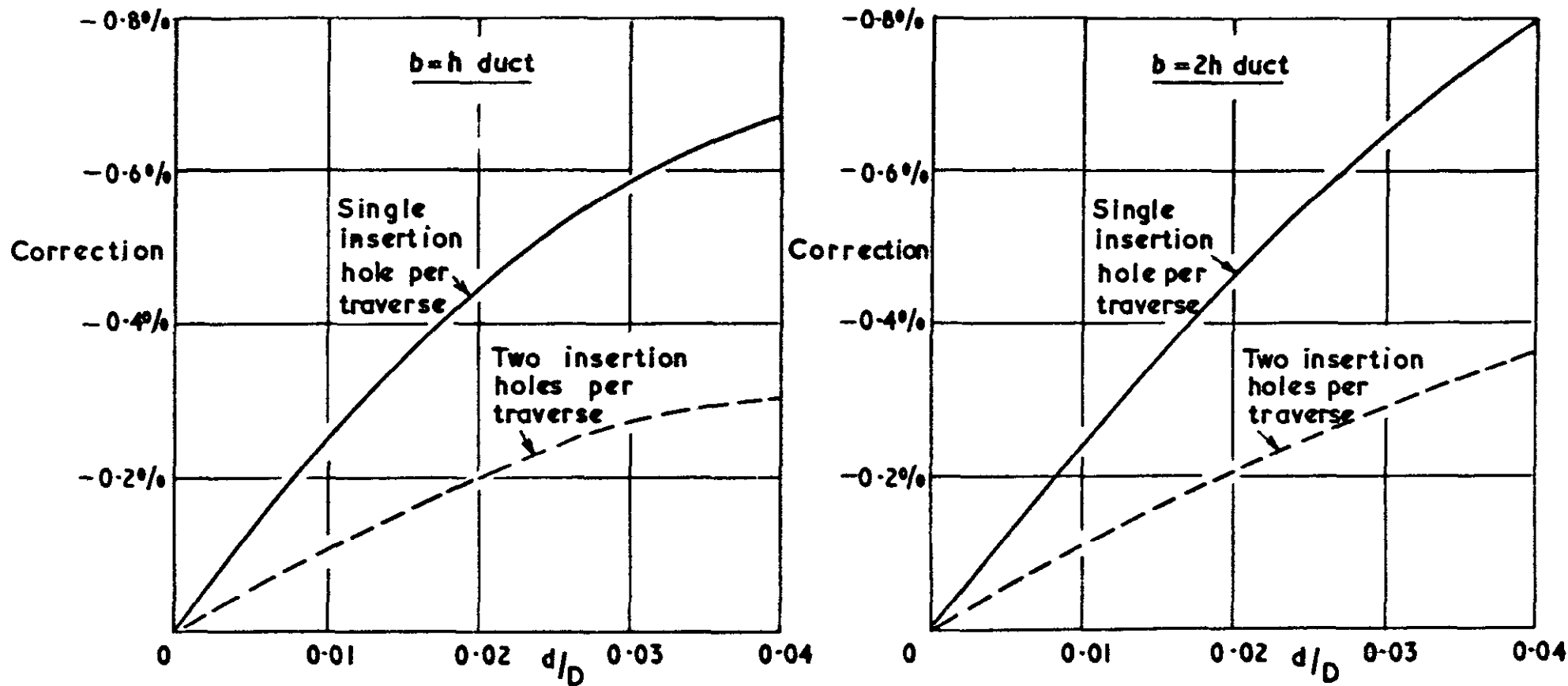


FIG 8

Pitot-stem blockage corrections to volume flow rate measured in rectangular ducts with an $x=8d$ pitot tube using the 26point log-linear method. (Stem parallel to side h)

© *Crown copyright* 1971

Produced and published by
HER MAJESTY'S STATIONERY OFFICE

To be purchased from
49 High Holborn, London WC1V 6HB
13a Castle Street, Edinburgh EH2 3AR
109 St Mary Street, Cardiff CF1 1JW
Brazennose Street, Manchester M60 8AS
50 Fairfax Street, Bristol BS1 3DE
258 Broad Street, Birmingham B1 2HE
80 Chichester Street, Belfast BT1 4JY
or through booksellers

Printed in England